



Published in final edited form as:

JACC Clin Electrophysiol. 2018 August ; 4(8): 1106–1114. doi:10.1016/j.jacep.2018.05.003.

Effects of Vagal Nerve Stimulation on Ganglionated Plexi Nerve Activity and Ventricular Rate in Ambulatory Dogs with Persistent Atrial Fibrillation

Zhaolei Jiang, MD^{1,2}, Ye Zhao, MD^{1,3}, Wei-Chung Tsai, MD^{1,4}, Yuan Yuan, MD^{1,2}, Kroekkiat Chinda, DVM, PhD^{1,5}, Jian Tan, MS¹, Patrick Onkka, MD¹, Changyu Shen, PhD⁶, Lan S. Chen, MD⁷, Michael C. Fishbein, MD⁸, Shien-Fong Lin, PhD^{1,9}, Peng-Sheng Chen, MD¹, and Thomas H. Everett IV, PhD.¹

¹Krannert Institute of Cardiology and Division of Cardiology, Department of Medicine, Indiana University School of Medicine, China ²Department of Cardiothoracic Surgery, Xinhua Hospital, Shanghai Jiaotong University School of Medicine, China ³Department of Cardiac Surgery, the First Affiliated Hospital of China Medical University, China ⁴Division of Cardiology, Department of Internal Medicine, Kaohsiung Medical University Hospital, Kaohsiung Medical University, Kaohsiung, Taiwan ⁵Department of Physiology, Faculty of Medical Science, Naresuan University, Phitsanulok, Thailand ⁶Richard and Susan Smith Center for Outcomes Research in Cardiology, Beth Israel Deaconess Medical Center, Harvard Medical School, Boston, MA ⁷Department of Neurology, Indiana University School of Medicine, David Geffen School of Medicine at UCLA ⁸Department of Pathology and Laboratory Medicine, David Geffen School of Medicine at UCLA ⁹Institute of Biomedical Engineering, National Chiao-Tung University, Hsin-Chu, Taiwan

Abstract

Objective—To test the hypothesis that low level vagal nerve stimulation (LL-VNS) reduces the ventricular rate (VR) during atrial fibrillation (AF) through the activation of the inferior vena cava-inferior atrial ganglionated plexus nerve activity (IVC-IAGPNA).

Background—Increased IVC-IAGPNA can suppress atrioventricular (AV) node conduction and slow VR in canine models of AF.

Methods—Persistent AF was induced in 6 dogs and the IVC-IAGPNA, right vagal nerve activity (RVNA), left vagal nerve activity (LVNA) and an electrocardiogram were recorded. After persistent AF was documented, VNS was programed to 14s ON and 1.1 min OFF. After 1 week, the VNS was reprogramed to 3 min OFF and stimulation continued for another week. Neural

Corresponding Author: Thomas H. Everett, IV, PhD, 1800 N. Capitol Ave, E400E, Indianapolis, IN 46202, Phone: 317-274-0957; theveret@iu.edu.

Potential Conflict of Interest: Shien-Fong Lin and Thomas H. Everett, IV have equity interest in Arrhythmotech, LLC. Cyberonics, Medtronic and St. Jude Medical Inc. donated research equipment to Dr. Chen's research laboratory.

Publisher's Disclaimer: This is a PDF file of an unedited manuscript that has been accepted for publication. As a service to our customers we are providing this early version of the manuscript. The manuscript will undergo copyediting, typesetting, and review of the resulting proof before it is published in its final citable form. Please note that during the production process errors may be discovered which could affect the content, and all legal disclaimers that apply to the journal pertain.

remodeling of the stellate ganglion (SG) was assessed with tyrosine hydroxylase (TH) staining and TUNEL staining.

Results—Average IVC-IAGPNA was increased during both VNS 1.1min OFF ($8.20 \pm 2.25 \mu\text{V}$ [95% CI, 6.33–9.53], $P=0.002$) and 3min OFF ($7.96 \pm 2.03 \mu\text{V}$ [95% CI, 6.30–9.27], $P=0.001$) versus baseline ($7.14 \pm 2.20 \mu\text{V}$ [95% CI, 5.35–8.52]). VR was reduced during both VNS 1.1min OFF ($123.29 \pm 6.29 \text{ bpm}$ [95% CI, 116.69–129.89], $P=0.001$) and 3min OFF ($120.01 \pm 4.93 \text{ bpm}$ [95% CI, 114.84–125.18], $P=0.001$) compared to baseline ($142.04 \pm 7.93 \text{ bpm}$ [95% CI, 133.72–150.37]). Abnormal regions were observed in the left SG, but not in the right SG. TUNEL-positive neurons were found in $22.2 \pm 17.2\%$ [95% CI, 0.9%–43.5%] of left SG cells and $12.8 \pm 8.4\%$ [95% CI, 2.4%–23.2%] of right SG cells.

Conclusions—Chronic LL-VNS increases IVC-IAGPNA and damages bilateral stellate ganglia. Both mechanisms could contribute to the underlying mechanism of VR control during AF.

Keywords

atrial fibrillation; neuromodulation; ganglionated plexi; stellate ganglion

Introduction

An increase in autonomic nerve activity has been associated with an increase in atrial arrhythmogenesis by correlating to the induction of atrial tachyarrhythmias such as atrial tachycardia (AT) and atrial fibrillation (AF).^(1–5) A change in autonomic nerve activity may be able to suppress these triggers and reduce the incidence of AF. Currently, low-level vagal nerve stimulation (LL-VNS) has been considered to be effective in suppressing AF induction and controlling ventricular rate (VR) during AF.^(6–9) However, the underlying mechanisms by which LL-VNS has a therapeutic effect of rate control during AF remains unclear. It has been previously demonstrated that left sided LL-VNS could damage the left stellate ganglion (SG), suppress stellate ganglion nerve activity (SGNA), and reduce the incidence of paroxysmal tachyarrhythmias (PAT) in ambulatory dogs.^(8,10) Those same effects could reduce sympathetic tone and help control the VR. However, studies have shown that atrioventricular (AV) nodal modulation that effects AV nodal conduction plays an important role in regulating the VR during AF.^(11–14) Direct electric stimulation of the inferior vena cava-inferior atrial ganglionated plexus (IVC-IAGP) has been effective in controlling VR.^(12–15) In our previous study, we demonstrated that the left vagal nerve controls the AV node in a majority of dogs during sustained AF, whereas the right vagal nerve controls the sinus node.^(1,14) Also, we found that left vagal nerve activity was associated with VR reduction when it co-activates with the inferior vena cava-inferior atrial ganglionated plexus nerve activity (IVC-IAGPNA).⁽¹⁴⁾ Whether or not LL-VNS can affect the IVC-IAGPNA remains unknown. The purpose of the present study was to investigate the changes of IVC-IAGPNA before and after LL-VNS in a canine model of AF to test the hypotheses that LL-VNS reduces VR via increases in IVC-IAGPNA.

Methods

The animal protocol was approved by the Institutional Animal Care and Use Committee of the Indiana University School of Medicine and the Methodist Research Institute, Indianapolis, IN, and conformed to the regulations for humane care and treatment of animals established by the NIH. A total of 6 mongrel dogs (23–28 kg) were studied.

Surgical procedures

For pacemaker and radiotransmitter implantation, a right thoracotomy was performed through the fourth intercostal space. Anesthesia was induced with ketamine (5–10 mg/kg) and midazolam (0.1–0.2 mg/kg IV), and after intubation and mechanical ventilation, anesthesia was maintained with 2.0% isoflurane. An epicardial pacing lead was implanted onto the right atrial appendage and connected to a subcutaneously positioned Medtronic Secura implantable pacemaker (Medtronic Inc, Minneapolis, MN) that was modified for high rate (600bpm) atrial pacing. A radiotransmitter (D70EEE, Data Sciences International, St. Paul, MN) with 3 bipolar recording electrodes was implanted to record nerve activity and an electrocardiogram (ECG).^(16,17) To record IVC-IAGPNA, electrodes were sutured onto the IVC-IAGP beneath its fascia. To record right vagal nerve activity (RVNA), electrodes were sutured onto the superior cardiac branch of the right vagal nerve. To record left vagal nerve activity (LVNA), electrodes were placed on the left cervical vagal nerve. For vagal nerve stimulation, a bipolar stimulating lead was implanted around the left cervical vagal nerve and connected to a subcutaneously positioned Cyberonics Demi-pulse neurostimulator (Cyberonics Inc, Houston, TX).

Pacing protocol

After 2 weeks of postoperative recovery, the DSI radiotransmitter was turned on to record baseline rhythm and nerve activity for 1 day. After 24 hours of recording, high-rate (600bpm, twice the diastolic threshold) atrial pacing was then initiated and continued for 2 weeks. After 2 weeks, the pacemaker was turned off to determine the presence of persistent AF (lasting >48 hours) (Figure 1).⁽⁷⁾ If persistent AF was present, the recording was continued for another 24 hours for simultaneous recording of the nerve activity and the ECG. If the dog was not in AF, the atrial pacing was reinitiated, and the ECG was monitored weekly until persistent AF was documented.

LL-VNS protocol

After the development of persistent AF, baseline nerve activity was recorded for 24 hours. Vagal nerve stimulation (VNS) was then initiated with the stimulator programmed to 14s ON and 1.1min OFF (10Hz, 500 μ s pulse duration) in all dogs based on the protocol in the ANTHEM-HF trial.⁽¹⁸⁾ The output current (mA) was progressively increased to 1.5 mA during the first 2 weeks of pacing, depending on the tolerability of VNS in each individual dog. An output current of 1.5 mA was chosen because it has previously been shown that an output current of 1.5 mA provided an effect on VR reduction during the OFF time.⁽¹⁹⁾ After 1 week of LL-VNS (1.5 mA, 14s ON, 1.1 min (short) OFF), the stimulator was turned off and the nerve activity and ECG were recorded for 24 hours. The stimulator was then programmed to 14s ON and 3 min (long) OFF to test the hypothesis that a longer off time

would have similar effects as the shorter off time. After another week of VNS (1.5 mA, 14s ON, 3 min OFF), the nerve activity and ECG were recorded again for 24 hours (Figure 1). The dog was then euthanized.

Immunohistochemistry Studies

Both left and right SG of all dogs were obtained and fixed in 4% formalin for 45 min, followed by storage in 70% alcohol. The tissues were processed routinely, paraffin embedded and cut into 5- μ m thick sections. Immunohistochemical staining was performed with antibodies against tyrosine hydroxylase (TH) using mouse monoclonal anti-TH (Accurate Chemical, Westbury, NY #BYA90291). Trichrome stains were performed on all specimens. All slides were examined manually under a BX60 microscope (Olympus, Tokyo, Japan) to determine if there were regions with decreased neuron cell density, pyknotic cell body, decreased TH staining and increased fibrosis. These regions of the SG were considered “abnormal” regions.(7) The size of the abnormal and normal regions was then determined with Image J software. A blinded observer reviewed randomly select 20X fields with the highest neuron cell density in both a normal region and an abnormal region. The mean number of neurons and the mean percentage of TH-negative neurons were compared between normal and abnormal regions in each SG.

To determine the neurotoxicity of LL-VNS to the bilateral SG, terminal deoxynucleotidyl transferase dUTP nick end labeling (TUNEL) staining was performed to detect the apoptotic cells (In Situ Cell Death Detection Kit, POD ref#11684817910; Sigma-Aldrich, St. Louis, MO). A blinded observer reviewed randomly select 40X fields with the highest neuron density in the bilateral SG. The mean percentage of TUNEL-positive neurons was compared between left SG and right SG.

Data analysis

The signals were manually analyzed using custom-written software to determine the temporal relationship between nerve activity and heart rate changes.(8) Data from RVNA or LVNA were high-pass filtered at 150Hz. Discrete wavelet filtering was used to remove the ECG components and obtain IVC-IAGPNA.(16) Nerve activity was considered present if there was an at least a 3-fold increase in the amplitude over baseline noise. Nerve activity from 2 different nerve structures was considered co-activated when the activation of the 2 nerve structures occurred simultaneously. A surface ECG was not directly recorded, however low-pass filtering (100Hz) was applied to the RVNA recording to obtain an ECG for VR and arrhythmia analysis.(20) To quantify the nerve activity, the average amplitude of the nerve activity was calculated over a 10-second window. Within each 10-second window, the filtered signals were then rectified, integrated with a 100-ms time constant, and summed to represent integrated nerve activity of the 10-s segment during the VNS OFF-time. The results were then divided by the total number of samples. RR-intervals were averaged over a 10-second window for a 24-hour period to construct the RR-interval distribution curve. A linear mixed-effects model was fitted to the RR-interval data where the different phases are treated as fixed effects and the animal was treated as random effects. The data were reported as mean \pm Standard Deviation (SD) and 95% confidence interval (CI). Paired *t* tests were performed to compare the differences between heart rate and integrated nerve activities at

different experimental time points. Independent *t* tests were performed to compare the differences between normal regions and abnormal regions or between left SG and right SG. A Pearson correlation coefficient was calculated between the percentage of TUNEL-positive neuron cell in the left SG and that in the right SG. A *P* value of 0.05 was considered statistically significant.

Results

All dogs completed the AF pacing protocol, and developed sustained AF after 4.0 ± 1.8 weeks (2~6 weeks) of rapid atrial pacing. The time to persistent AF did not correlate with VR or nerve activity. The *r* values were 0.367 (*p*=0.475), -0.383 (*p*=0.454), -0.458 (*p*=0.361) and 0.585 (*p*=0.222) for nerve activity on IVC-IAGPNA, RVNA, LVNA and for heart rate, respectively. Termination of persistent AF was not observed during VNS pacing.

Effects of LL-VNS on Integrated Nerve Activity

LVNA, RVNA and IVC-IAGPNA were analyzed at baseline, after the establishment of persistent AF (AF baseline), and during LL-VNS for each dog (Table 1). The establishment of persistent AF significantly increased the measured nerve activity in all measured parameters except LVNA. However, LL-VNS increased the vagal nerve activity as the average LVNA was significantly increased at the short OFF period compared to AF baseline. Even though there was no significant difference between the short and long OFF periods, the nerve activity measured during the long OFF period was not significantly different from that measured at AF baseline. LL-VNS also increased the average RVNA at both the short and long OFF periods, however the increase in activity was not significantly different from the nerve activity measured during AF.

A significant increase in IVC-IAGPNA was measured following the initiation of persistent AF. However, compared with the nerve activity measured at AF baseline, IVC-IAGPNA was further increased during the short and long OFF periods in all 6 dogs. Similar to RVNA and LVNA, there was no significant difference in average IVC-IAGPNA between VNS short and long OFF periods (*P*=0.268).

Figure 2 shows an example of simultaneous LVNA, RVNA and IVC-IAGPNA discharges. There was transient VR acceleration in the beginning of these discharges. However, persistent IVC-IAGPNA discharges were associated with a markedly reduced VR. The vagal nerves are known to have significant sympathetic components and the vagal nerve activations may sometimes be associated with heart rate acceleration in sinus rhythm.⁽²¹⁾ Therefore, the initial VR acceleration suggests the activation of the sympathetic component of the vagal nerves. After the initial activation, the continued nerve activity is typically associated with VR reduction. The figure also shows that IVC-IAGPNA continued to occur after RVNA withdrawal. The continued elevation of IVC-IAGPNA was associated with reduced sinus rate. These findings suggest that intrinsic cardiac nerve activity may independently reduce the sinus rate in the absence of continued vagal discharges. Similar types of activation were also observed during AF as co-activation of LVNA and IVC-IAGPNA correlated to a slowing of the VR as shown in Figure 3. The figure also shows that IVC-IAGPNA continued to occur after LVNA withdrawal. As the summary data in Table 1

shows, both LVNA and RVNA increased during LL-VNS pacing. Figure 4 shows an example of the characteristic nerve activity with LL-VNS. IVC-IAGP co-activated with the onset of LL-VNS and continued to discharge after LL-VNS terminated. Also as the figure shows, VR deceleration immediately occurred after LL-VNS termination.

Effects of LL-VNS on Ventricular Rate during AF

As shown in Table 1, the VR significantly increased during AF compared to sinus rhythm. The VR was significantly reduced during both VNS short and long OFF periods compared to AF baseline. In addition, the reduction of VR during the long OFF period was greater than that of the short OFF period ($P=0.039$). Figure 4 shows a typical example of VR change during LL-VNS. VR didn't significantly change during LL-VNS, but VR deceleration occurred immediately after LL-VNS terminated at a time when LVNA returned to baseline, but elevated IVC-IAGP was sustained. The average percentage of RR intervals were also determined and plotted the average distribution for all 6 dogs (Figure 5). Compared with sinus baseline, most RR intervals were shorter than 0.5s during AF without VNS. The curve associated with the short and long OFF periods shifted to the right, as the RR intervals during VNS pacing became longer than that of AF baseline.

Effects of LL-VNS on Neural Remodeling of Bilateral SG in Sustained AF

Bilateral SGs were available for analyses from 5 of 6 dogs. Abnormal regions were found in the left SG of all 5 available SG, but abnormal regions were not visible in the right SG using light microscopy. In the left SG, the size of the abnormal region accounted for $38.6\pm 19.3\%$ [95% CI, 14.7% to 62.5%] of the visible area. Figure 6 shows an example of an abnormal region in the left SG from one dog. Within the abnormal region, neuron cell density was decreased, TH staining was weaker, cell bodies were pyknotic and fibrosis was increased. Compared with a normal region of the left SG (139.0 ± 19.3 [95% CI, 115.1 to 162.9]), mean neuron cell number was significantly decreased in the abnormal region (115.6 ± 7.3 [95% CI, 106.6 to 124.7]) ($P=0.035$). The mean percentage of TH-negative neuron cells in the abnormal region ($8.4\pm 4.1\%$ [95% CI, 3.3% to 13.6%]) was significantly higher than that in normal region ($3.0\pm 1.3\%$ [95% CI, 0% to 6.5%]) ($P=0.04$). Figure 7 shows that TUNEL-positive cells were observed in both neuron and non-neuron cells in both left SG and right SG of all 5 available dogs. In the left SG, the mean percentage of TUNEL-positive neuron cells was $22.2\pm 17.2\%$ [95% CI, 0.9% to 43.5%]. In the right SG, the mean percentage of TUNEL-positive neuron cells was $12.8\pm 8.4\%$ [95% CI, 2.4% to 23.2%]. While there was no significant difference between left SG and right SG ($P=0.303$), the percentage of TUNEL-positive neurons in the right SG was at or below the mean in 4 of the 5 dogs (Figure 8).

Discussion

This study demonstrated that chronic LL-VNS increases IVC-IAGPNA which correlated to reduced VR in ambulatory dogs with pacing induced sustained AF. In addition, chronic LL-VNS resulted in bilateral stellate ganglionic cell death, although grossly abnormal regions were observed only in the LSG. These changes could also help to control VR during AF by reducing the sympathetic outflow to the heart. These findings indicate that increasing IVC-

IAGPNA and the corresponding neural remodeling of the bilateral SG may be the underlying mechanism of the rate control effect of LL-VNS during sustained AF.

In a previous study in which we monitored IVC-IAGP and vagal nerve activity in ambulatory dogs with persistent AF, the IVC-IAGPNA was associated with VR reduction during AF.(14) Right or left VNA was associated with VR reduction only when it co-activated with the IVC-IAGPNA. Previous studies have also shown that in ambulatory dogs with persistent AF, the density of tyrosine hydroxylase-positive nerve was reduced in dogs receiving LL-VNS as compared with a control group that did not have VNS.(7,8) These studies were used as a control for the current study.

Chronic LL-VNS Increases IVC-IAGPNA and Reduces Ventricular Rate

Activity within both the extrinsic cardiac nervous system (ECNS) and the intrinsic cardiac nervous system (ICNS) is known to be related to an increase in atrial arrhythmogenesis.(1,2) Choi et al.(2) showed that there was a significant temporal relationship between extrinsic cardiac nerve activity (ECNA; including stellate ganglion nerve activity and vagal nerve activity) and intrinsic nerve activity (ICNA; including epicardial ganglionated plexi nerve activity and ligament of Marshall nerve activity), indicating communication between ECNS and ICNS. Stimulating the ECNS via VNS has been shown to be effective in suppressing the occurrence of AF and reducing VR during persistent AF.(7–10) In addition, Chinda et al.(7) also found that intermittent VNS with short ON-time (14 seconds) and long OFF-time (66 seconds) could lead to reduced SGNA and VR control during persistent AF. These studies revealed that VNS could inhibit arrhythmogenesis by controlling ECNS.

The IVC-IAGP has been shown to be important in modulating AV node conduction as IVC-IAGP activity correlated to slow VR.(13,22,23) Park et al.(14) demonstrated that IVC-IAGPNA and VNA often discharged together and was associated with VR reduction during AF. However, whether LL-VNS could affect IVC-IAGPNA during AF in ambulatory dogs has not been shown. In this study, we directly recorded IVC-IAGPNA and VR in ambulatory dogs with persistent AF before and during LL-VNS. We found that chronic LL-VNS increased IVC-IAGPNA and reduced VR within this ambulatory dog model. Before LL-VNS, IVC-IAGPNA showed a weak correlation with LVNA. However, when LL-VNS was on, IVC-IAGPNA was often activated by LL-VNS and continued to discharge after LL-VNS terminated. In addition, VR deceleration immediately occurred after LL-VNS terminated. VR deceleration was shown to be related to increasing IVC-IAGPNA during persistent AF. Both VNS with the short and long OFF periods significantly increased IVC-IAGPNA and reduced VR during AF. The reduction of the VR during VNS with the longer OFF period was significantly greater than the shorter OFF period, but there was no significant difference in IVC-IAGPNA. LL-VNS increasing IVC-IAGPNA may be one of mechanisms that VNS reduces VR during persistent AF.

Neurotoxicity of Chronic LL-VNS on the Bilateral SG

Studies involving LL-VNS have shown that the effects include suppressing left stellate ganglion nerve activity, a reduction in the incidence of PAT in ambulatory dogs,(8) and a reduction in VR during persistent AF.(7) These studies showed that LL-VNS caused neural

remodeling of the LSG with a decreased density of TH-positive nerves and more neurons without immunoreactivity to TH. In this study, obvious signs of abnormal regions were observed in the left SG and TUNEL-positive neuron cells were found in both left SG and right SG. These results demonstrate that chronic LL-VNS induces bilateral stellate ganglion cell death. The damage to the left SG appeared to be more apparent than that of right SG, although the differences were not statistically significant. The mechanism may be that cervical vagus nerves contain both sympathetic and parasympathetic nerve fibers, so there is direct neural communication between the vagal nerve and the sympathetic trunk.(21,24) Chronic stimulation of the sympathetic component within the vagal nerve may not only suppress SG nerve activity, but also cause SG cell death (neurotoxicity) due to intracellular calcium accumulation.(25)

Study limitations

A limitation of the study is that we did not directly record the SGNA. In addition, we only observed the effect of left side LL-VNS. VNS with 1.1 min OFF was always performed first. It is not known if neurotoxicity occurred during this pacing such that continued VNS pacing with 3 min OFF showed a greater reduction in VR. Within the nerve recording, afferent and efferent nerve activity cannot be differentiated.

Conclusions

This study has shown that LL-VNS effects the heart rate during persistent AF. Chronic LL-VNS increases IVC-IAGPNA and induces bilateral stellate ganglionic cell apoptosis. These resulting effects of LL-VNS contribute to the underlying mechanism of VR control during AF.

Acknowledgments

Funding Sources: This study was supported in part by NIH Grants R42DA043391 (Dr Everett), P01 HL78931, R56 HL71140, R01 HL71140, U18 TR002208-01, R01 HL139829 (Dr Chen), a Charles Fisch Cardiovascular Research Award endowed by Dr Suzanne B. Knoebel of the Krannert Institute of Cardiology (Dr Everett), a Medtronic-Zipes Endowment and the Indiana University Health-Indiana University School of Medicine Strategic Research Initiative (Dr Chen).

Abbreviations

AF	atrial fibrillation
ECNA	extrinsic cardiac nerve activity
ECNS	extrinsic cardiac nervous system
ICNA	intrinsic cardiac nerve activity
ICNS	intrinsic cardiac nervous system
IVC-IAGP	inferior vena cava-inferior atrial ganglionated plexus
IVC-IAGPNA	inferior vena cava-inferior atrial ganglionated plexus nerve activity

LL-VNS	low level vagal nerve stimulation
LVNA	left vagal nerve activity
RVNA	right vagal nerve activity
SG	stellate ganglion
SGNA	stellate ganglion nerve activity
TH	tyrosine hydroxylase
VNA	vagus nerve activity
VR	ventricular rate

References

1. Chen PS, Chen LS, Fishbein MC, Lin SF, Nattel S. Role of the autonomic nervous system in atrial fibrillation: pathophysiology and therapy. *Circ Res*. 2014; 114:1500–15. [PubMed: 24763467]
2. Choi EK, Shen MJ, Han S, et al. Intrinsic cardiac nerve activity and paroxysmal atrial tachyarrhythmia in ambulatory dogs. *Circulation*. 2010; 121:2615–23. [PubMed: 20529998]
3. Park HW, Shen MJ, Lin SF, Fishbein MC, Chen LS, Chen PS. Neural mechanisms of atrial fibrillation. *Curr Opin Cardiol*. 2012; 27:24–8. [PubMed: 22139702]
4. Shen MJ, Zipes DP. Role of the autonomic nervous system in modulating cardiac arrhythmias. *Circ Res*. 2014; 114:1004–21. [PubMed: 24625726]
5. Tan AY, Zhou S, Ogawa M, et al. Neural mechanisms of paroxysmal atrial fibrillation and paroxysmal atrial tachycardia in ambulatory canines. *Circulation*. 2008; 118:916–25. [PubMed: 18697820]
6. Chen M, Yu L, Zhou X, Liu Q, Jiang H, Zhou S. Low-level vagus nerve stimulation: an important therapeutic option for atrial fibrillation treatment via modulating cardiac autonomic tone. *Int J Cardiol*. 2015; 199:437–8. [PubMed: 26263011]
7. Chinda K, Tsai WC, Chan YH, et al. Intermittent left cervical vagal nerve stimulation damages the stellate ganglia and reduces the ventricular rate during sustained atrial fibrillation in ambulatory dogs. *Heart Rhythm*. 2016; 13:771–80. [PubMed: 26607063]
8. Shen MJ, Shinohara T, Park HW, et al. Continuous low-level vagus nerve stimulation reduces stellate ganglion nerve activity and paroxysmal atrial tachyarrhythmias in ambulatory canines. *Circulation*. 2011; 123:2204–12. [PubMed: 21555706]
9. Stavrakis S, Humphrey MB, Scherlag BJ, et al. Low-level transcutaneous electrical vagus nerve stimulation suppresses atrial fibrillation. *J Am Coll Cardiol*. 2015; 65:867–75. [PubMed: 25744003]
10. Shen MJ, Hao-Che C, Park HW, et al. Low-level vagus nerve stimulation upregulates small conductance calcium-activated potassium channels in the stellate ganglion. *Heart Rhythm*. 2013; 10:910–5. [PubMed: 23357541]
11. Kornet L, van Hunnik A, Michels K, et al. Stimulation of the intra-cardiac vagal nerves innervating the AV-node to control ventricular rate during AF: specificity, parameter optimization and chronic use up to 3 months. *J Interv Card Electrophysiol*. 2012; 33:7–18. [PubMed: 21969125]
12. Bianchi S, Rossi P, Schauerte P, et al. Increase of ventricular interval during atrial fibrillation by atrioventricular node vagal stimulation: chronic clinical atrioventricular-nodal stimulation download study. *Circ Arrhythm Electrophysiol*. 2015; 8:562–8. [PubMed: 25878323]
13. Hou Y, Scherlag BJ, Lin J, et al. Ganglionated plexi modulate extrinsic cardiac autonomic nerve input: effects on sinus rate, atrioventricular conduction, refractoriness, and inducibility of atrial fibrillation. *J Am Coll Cardiol*. 2007; 50:61–8. [PubMed: 17601547]

14. Park HW, Shen MJ, Han S, et al. Neural control of ventricular rate in ambulatory dogs with pacing-induced sustained atrial fibrillation. *Circ Arrhythm Electrophysiol.* 2012; 5:571–80. [PubMed: 22586260]
15. Rossi P, Bianchi S, Barretta A, et al. Post-operative atrial fibrillation management by selective epicardial vagal fat pad stimulation. *J Interv Card Electrophysiol.* 2009; 24:37–45. [PubMed: 18758932]
16. Jiang Z, Zhao Y, Doytchinova A, et al. Using skin sympathetic nerve activity to estimate stellate ganglion nerve activity in dogs. *Heart Rhythm.* 2015; 12:1324–32. [PubMed: 25681792]
17. Robinson EA, Rhee KS, Doytchinova A, et al. Estimating sympathetic tone by recording subcutaneous nerve activity in ambulatory dogs. *J Cardiovasc Electrophysiol.* 2015; 26:70–8. [PubMed: 25091691]
18. Premchand RK, Sharma K, Mittal S, et al. Autonomic regulation therapy via left or right cervical vagus nerve stimulation in patients with chronic heart failure: results of the ANTHEM-HF trial. *J Card Fail.* 2014; 20:808–16. [PubMed: 25187002]
19. Chinda K, Tsai WC, Chan YH, et al. Intermittent Left Cervical Vagal Nerve Stimulation Damages the Stellate Ganglia and Reduces Ventricular Rate During Sustained Atrial Fibrillation in Ambulatory Dogs. *Heart Rhythm.* 2016; 13:771–80. [PubMed: 26607063]
20. Tan AY, Zhou S, Ogawa M, et al. Neural mechanisms of paroxysmal atrial fibrillation and paroxysmal atrial tachycardia in ambulatory canines. *Circulation.* 2008; 118:916–925. [PubMed: 18697820]
21. Onkka P, Maskoun W, Rhee KS, et al. Sympathetic nerve fibers and ganglia in canine cervical vagus nerves: localization and quantitation. *Heart Rhythm.* 2013; 10:585–91. [PubMed: 23246597]
22. Hou Y, Scherlag BJ, Lin J, et al. Interactive atrial neural network: Determining the connections between ganglionated plexi. *Heart Rhythm.* 2007; 4:56–63. [PubMed: 17198991]
23. Rossi P, Ricci A, De Paulis R, et al. Epicardial ganglionated plexus stimulation decreases postoperative inflammatory response in humans. *Heart Rhythm.* 2012; 9:943–50. [PubMed: 22306617]
24. Seki A, Green HR, Lee TD, et al. Sympathetic nerve fibers in human cervical and thoracic vagus nerves. *Heart Rhythm.* 2014; 11:1411–7. [PubMed: 24768897]
25. Jaiswal MK, Zech WD, Goos M, et al. Impairment of mitochondrial calcium handling in a mtSOD1 cell culture model of motoneuron disease. *BMC Neurosci.* 2009; 10:64. [PubMed: 19545440]

Perspectives

Competency in Medical Knowledge

Currently, low-level vagal nerve stimulation (LL-VNS) has been considered to be effective in suppressing AF induction and controlling ventricular rate (VR) during AF. However, the underlying mechanisms by which LL-VNS has a therapeutic effect of rate control during AF remains unclear. The results of this study suggest that LL-VNS increases the inferior vena cava-inferior atrial ganglionated plexus nerve activity which can affect AV nodal conduction and decrease the VR.

Translational Outlook

Neuromodulation therapy including vagal nerve stimulation has been used for controlling arrhythmias and ventricular rate. However, the mechanisms of neuromodulation therapy are poorly understood. Understanding the mechanisms can help fill the knowledge gap in determining how the extrinsic nervous system can control the heart rate and help in assessing the efficacy of neuromodulation.

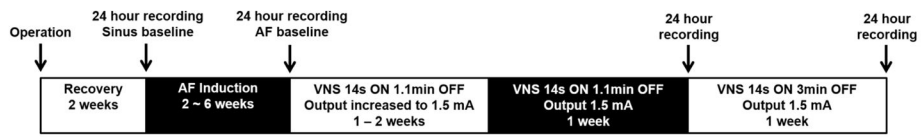


Figure 1. Study protocol. After 2 weeks of recovery, AF was induced by rapid atrial pacing. After persistent AF was achieved, chronic low-level vagal nerve stimulation (LL-VNS) was performed in all dogs.

Author Manuscript

Author Manuscript

Author Manuscript

Author Manuscript

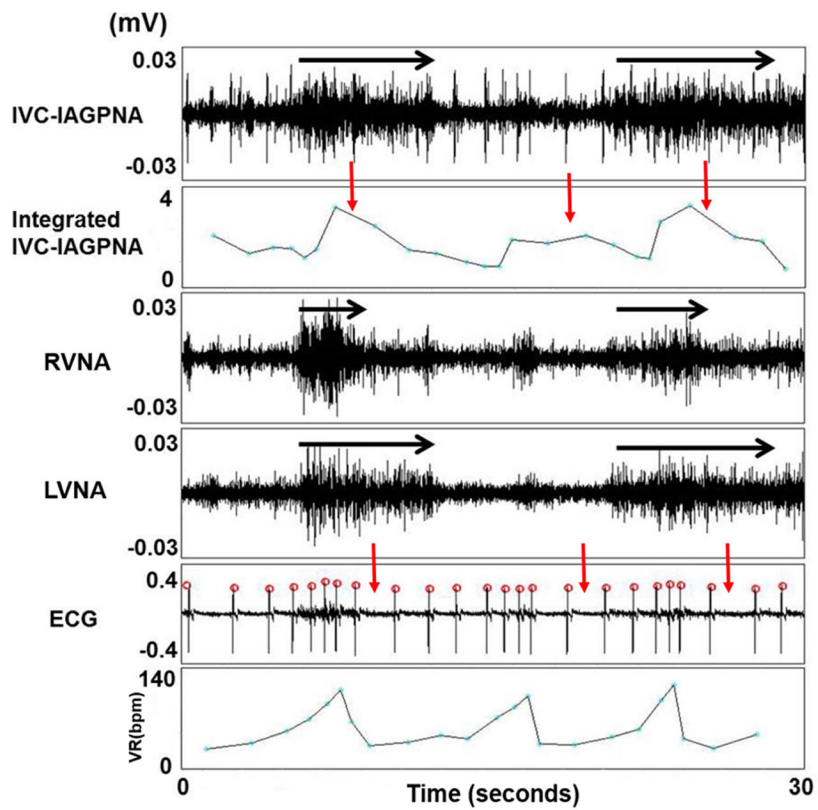


Figure 2. The relationship between LVNA and IVC-IAGPNA at sinus baseline. Simultaneous LVNA, RVNA and IVC-IAGPNA discharges were associated with initial VR acceleration, while continued discharges were associated with markedly suppressed VR. The black arrows indicate the event of significant nerve discharge. The red arrows highlight the integrated IVC-IAGP activity and its association with VR reduction.

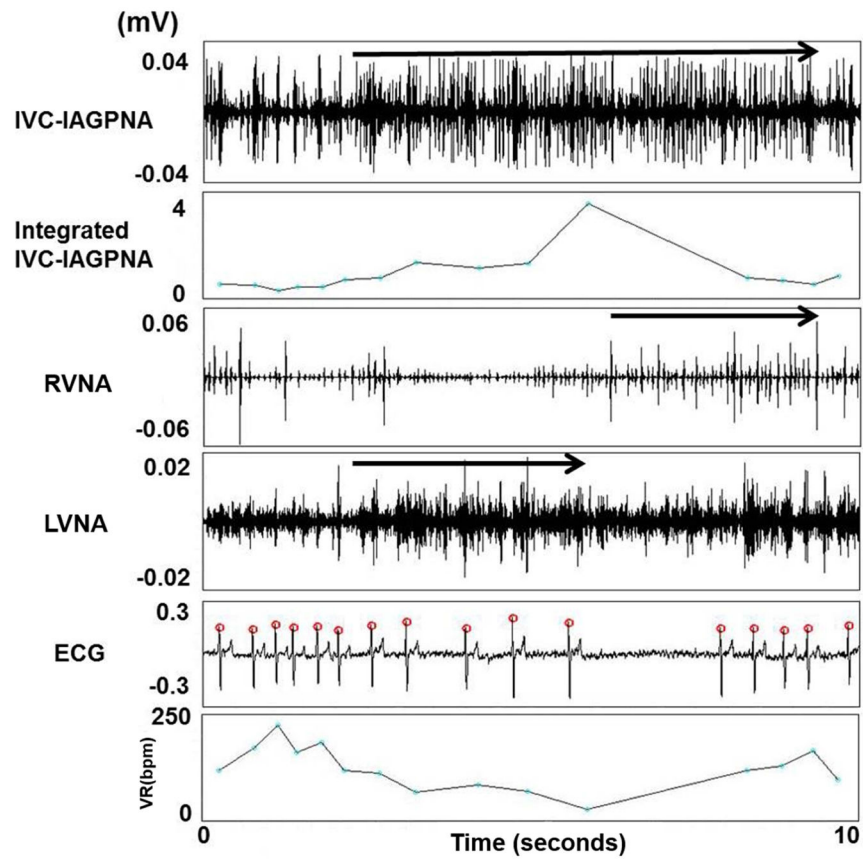


Figure 3. The relationship between LVNA and IVC-IAGPNA at AF baseline. Co-activation of LVNA and IVC-IAGPNA was correlated with a slowing of the VR during AF and IVC-IAGP continued to discharge after LVNA withdrawal. The arrows indicate the event of significant nerve discharge.

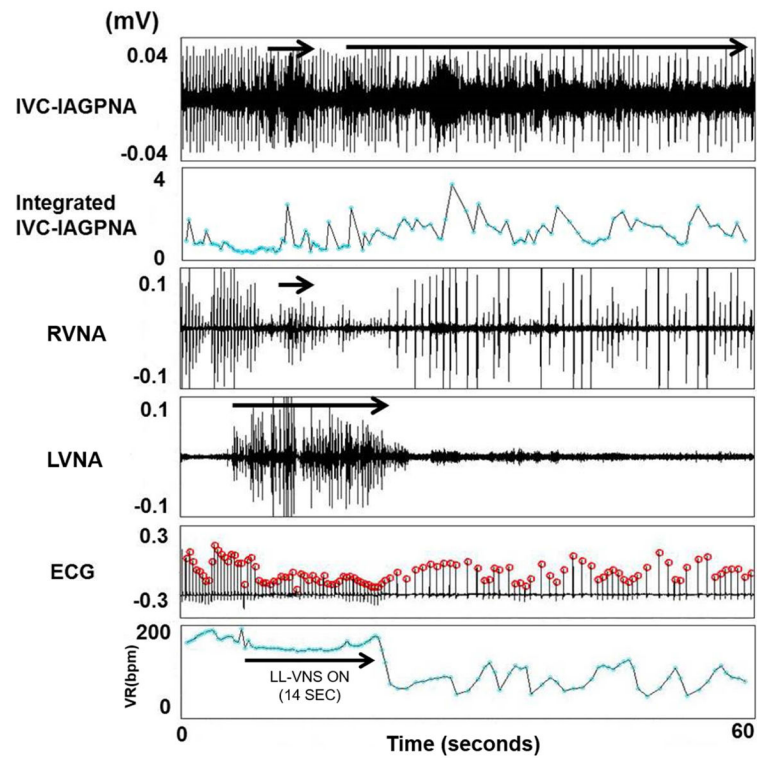


Figure 4.

The relationship between LVNA and IVC-IAGPNA during VNS 1.1 min OFF in a canine with persistent AF. Both LVNA and RVNA were activated when LL-VNS was on, but the change in RVNA was not as dramatic as LVNA. IVC-IAGP co-activated with LL-VNS and continued to discharge after LL-VNS terminated. Also, VR deceleration immediately occurred after LL-VNS terminated and appears to correlate with the continued elevation in IVC-IAGPNA. The arrows indicate the event of significant nerve discharge. The ECG is obtained from the electrodes that were placed on the vagal nerve. The red circles on top of each ECG are markers indicating the peak of the QRS complexes recognized by the computer. The times of those red circles were used for RR interval calculations.

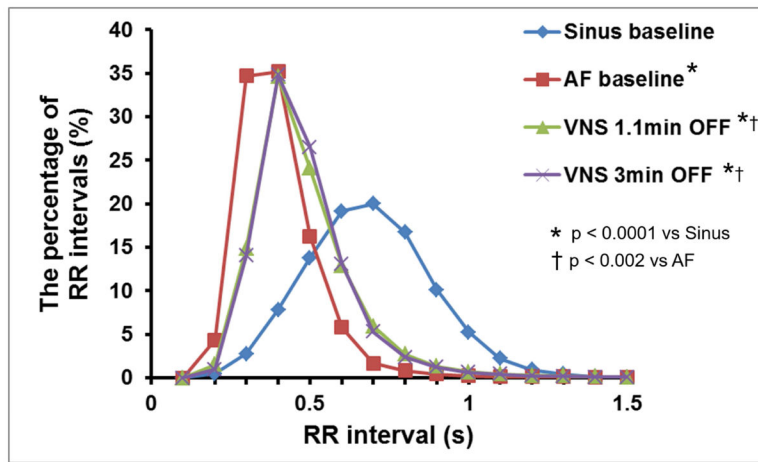


Figure 5. RR interval distribution at distinct stages of the experiment. Compared with sinus baseline, most RR intervals were shorter than 0.5s during AF without VNS. The curve of VNS 1.1 min OFF and VNS 3 min OFF shifted to the right, as the RR intervals during VNS 1.1 min OFF or VNS 3 min OFF became longer than that of AF baseline. The p-values are for the comparisons of the mean RR intervals among the four groups.

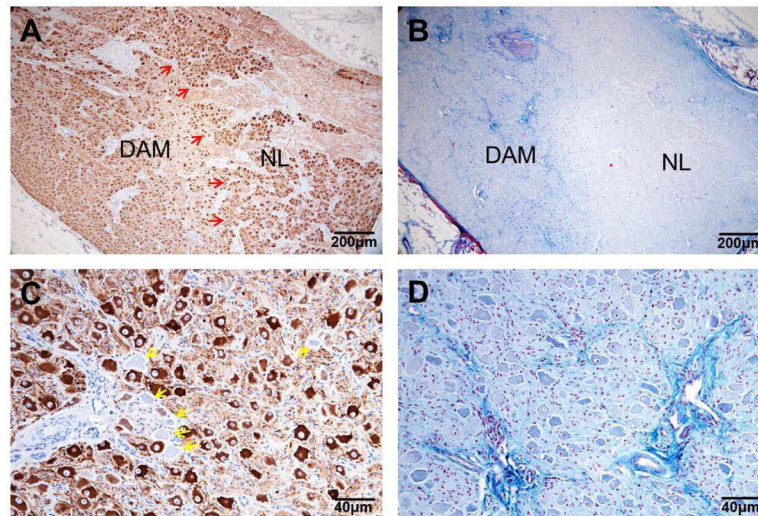


Figure 6. Histology of LSG with TH staining and Masson-Trichrome staining. A). TH immunostaining of the LSG at low magnification (4× objective lens) shows the presence of both a DAM and a NL in the same LSG. In the DAM of the LSG, it was observed that neuron cell density was decreased, TH staining was weaker. B). Masson-Trichrome staining of the same LSG (4× objective lens). The DAM of the LSG had increased fibrosis (blue). C). Higher power view (20× objective lens) of TH staining at the DAM of the LSG. Arrows point to neurons that did not stain for TH (TH-negative). Also, the cell body was pyknotic. D). High power view (20× objective lens) of the DAM with increased fibrosis (blue). DAM = damaged (abnormal) region; LSG = left stellate ganglion; NL = normal region; TH = tyrosine hydroxylase.

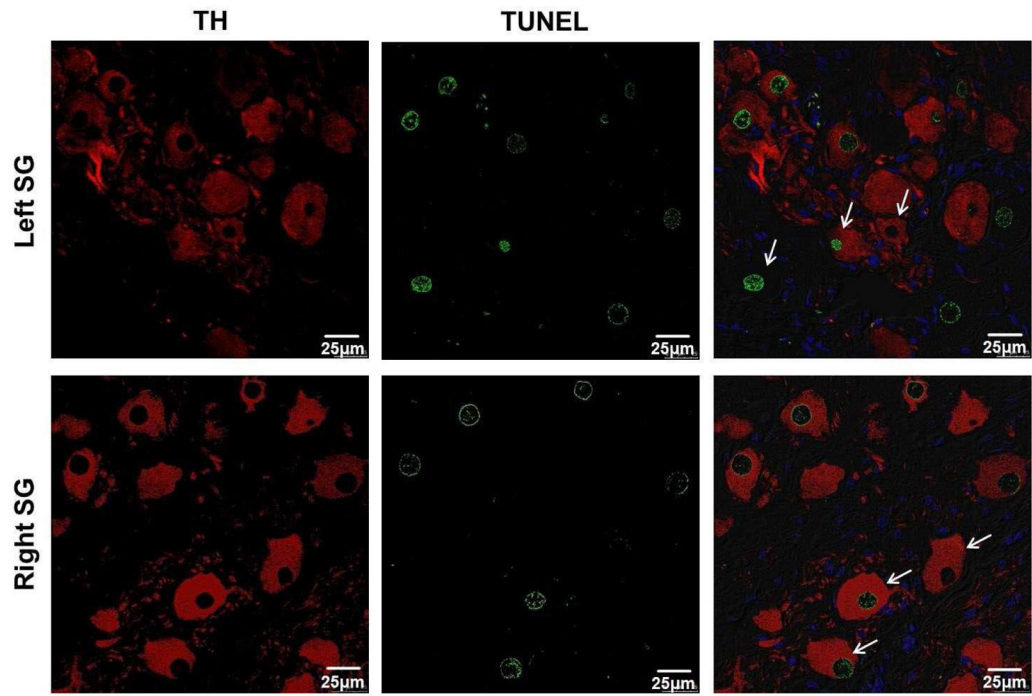


Figure 7. Confocal images of both TH and TUNEL staining for bilateral stellate ganglion. TUNEL-positive neuron cells were found in both left SG and right SG. *Green* indicates positive TUNEL stain. *Red* indicates positive TH stain. *Blue* is the DAPI stain of the nuclei.

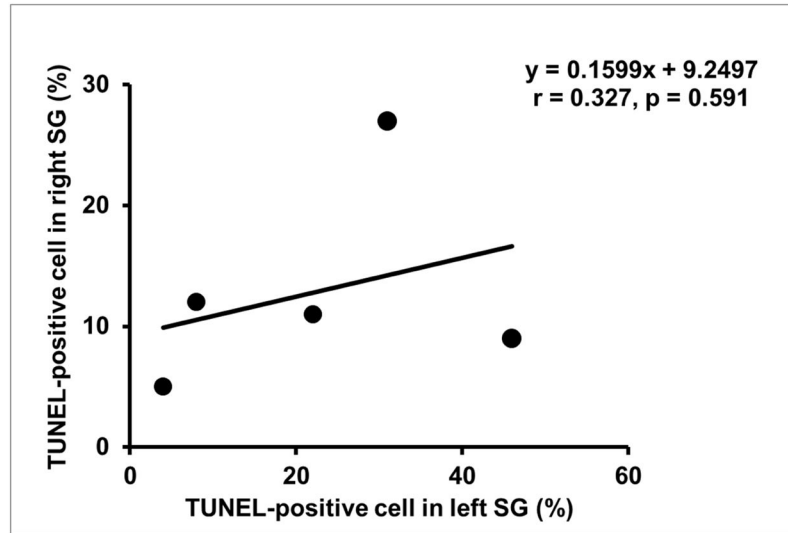


Figure 8. The correlation between the percentage of TUNEL-positive neurons in left SG and that in right SG. While TUNEL-positive neurons were observed in both the left SG and right SG, the left SG showed an increase in the variability of the percentage of positively stained cells.

Table 1

The effects of LL-VNS on LVNA, RVNA, IVC-IAGPNA and VR.

Parameter	Sinus baseline	AF baseline	VNS with 1.1min OFF	VNS with 3min OFF
IVC-IAGPNA(μ V)	2.60 \pm 1.12	7.14 \pm 2.20 [*]	8.20 \pm 2.25 ^{*Δ}	7.96 \pm 2.03 ^{*Δ}
LVNA(μ V)	1.92 \pm 0.72	2.19 \pm 0.67	2.65 \pm 0.75 ^{*Δ}	2.34 \pm 0.51 [*]
RVNA(μ V)	2.13 \pm 1.27	3.94 \pm 2.29 [*]	4.57 \pm 2.42 [*]	4.75 \pm 2.45 [*]
VR(beats/min)	87.60 \pm 10.04	142.04 \pm 7.93 [*]	123.29 \pm 6.29 ^{*Δ}	120.01 \pm 4.93 ^{*$\Delta$$\blacktriangle$}

* $P < 0.05$, vs Sinus baseline; Δ $P < 0.05$, vs AF baseline; \blacktriangle $P < 0.05$, vs VNS with 1.1 min OFF.